

Effects of Papillary Muscle Position on Chordal Force Distribution: An In-vitro Study

Jorge Hernan Jimenez, Dennis Dam Soerensen, Zhaoming He, Jennifer Ritchie, Ajit P. Yoganathan

Wallace H. Coulter Department of Biomedical Engineering, Georgia Institute of Technology & Emory University, Atlanta, GA, USA

Background and aim of the study: Mitral insufficiency, a common and morbid pathology, has been related to topological changes in the left ventricle. These changes may affect mitral leaflet coaptation by displacing the tips of the papillary muscles (PMs), subsequently changing the tension distribution on the chordae tendineae. Therefore, further understanding of the effects of PM displacement on chordal force distribution is required.

Methods: Six human and five porcine mitral valves were studied in a physiological left heart simulator. Cardiac output and transmitral pressure were recorded online and maintained within physiological ranges. Force transducers were placed on six chordae tendineae to measure chordal force distribution. Tension on individual chordae tendineae was recorded online during the cardiac cycle. The experiment was conducted for eight different PM positions, which were constructed from 5-mm vectorial displacements from the normal PM position.

Results: The anterior strut chord showed significant ($p < 0.05$) variations in peak systolic tension (PST) for

those positions associated with apical motion of the PMs. The posterior intermediate chord also showed significant variations in PST for positions associated with apical displacement of the PMs, whereas posterior displacement of the PMs resulted in a reduction in tension. In contrast, both the anterior marginal and posterior marginal chords showed a relatively uniform PST for the eight different PM positions. The posterior basal and commissural chords were the most sensitive to tension variations due to PM displacement. These chords showed relatively large and significant ($p < 0.05$) variations in PST for most of the different PM displacements.

Conclusion: The effects of PM relocation on chordal tension depended on chordal type. Chords which insert closer to the annulus were more sensitive to PM displacement, whereas those further from the annulus, the marginal chords, were the least sensitive to PM displacement.

The Journal of Heart Valve Disease 2005;14:295-302

Although mitral leaflet malcoaptation is the endpoint through which mitral regurgitation occurs (1), several topological changes within the left ventricle have been associated with mitral valve malfunction (2). Ventricular dilation (3-6) and sphericity (7-9), papillary muscle (PM) contractile malfunction (10), and motion abnormalities of the left ventricle have been associated with leaflet malcoaptation and therefore mitral regurgitation.

Alterations in the geometry or motion of the left ventricle result in repositioning of the PMs within the

mitral apparatus. Recent studies both in animal models (6,10) and human subjects (11) have quantified displacement of the PMs in pathologies such as ischemic mitral regurgitation and dilated cardiomyopathy. The results have shown that even subtle alterations in the position of the PMs during the cardiac cycle may lead to leaflet malcoaptation. Surgeons and clinicians have proposed several procedures to correct mitral regurgitation due to PM displacement. One solution is to reshape the ventricle (12,13), but this requires extensive surgical manipulation. Another proposed procedure is based on cutting a limited number of chords which have severely altered tension configurations in order to restore some degree of valve function (14). In addition, after chordal failure, valve repair may be accomplished through chordal replacement using sutures or chordal translocation. As the effects of PM repositioning are transmitted to the leaflets through

Address for correspondence:

Prof. Ajit P. Yoganathan, School of Biomedical Engineering & Petit Institute for Bioengineering and Bioscience, 317 Ferst Drive, Georgia Institute of Technology, Room 2119, Whitaker Building, Atlanta, GA 30332, USA

e-mail: ajit.yoganathan@bme.gatech.edu

the chordae tendineae, in order to restore valve function in pathological conditions which result in PM displacement, it is necessary to understand the interaction between PM position and chordal force distribution.

The study aim was to characterize the force on six representative mitral chordae tendineae under controlled variations in PM position in order to better understand mitral valve insufficiency in pathologies which induce PM relocation or discoordination. The intent was to provide a fundamental understanding of mitral valve function under physiological and pathological conditions, and to aid surgeons in the design of mitral repair procedures.

Materials and methods

Mitral valves

Fresh mitral valves (five porcine from a local abattoir, two human from Emory University, and four human provided by Corazon Technologies Inc., CA, USA) were used in the study. The hearts from Emory University were obtained from heart transplant recipients with Institutional Review Board approval following the guidelines for the protection of study volunteers in research. Valves with normal anatomical features and similar orifice areas ($6.8 \pm 0.3 \text{ cm}^2$) were used. The valves were extracted from the hearts, preserving the complete mitral apparatus, and preserved in saline solution (0.9%) during preparation and instrumentation. Using a flat annulus board, the mitral valves were mounted in the Georgia Tech left heart simulator using previously published methodologies (15-17). During suturing, special attention was placed on preserving the annular perimeter to avoid dilation or contraction.

In-vitro flow loop

The in-vitro experiments were carried out in the modified Georgia Tech left heart simulator. This system is capable of physiological and pathophysiological flow and pressure waveforms, and has been described in detail elsewhere (15-17).

Strain gauge transducers and force rods

C-ring force transducers were used to measure the tension on individual chordae tendineae. The sensitivity of these transducers (ca. 0.5 N/V) and linearity (0-5 N) were tested prior to and after each experiment. Details of C-ring construction and function have been published previously (16,18).

The left heart simulator uses force rods which attach to the PMs, enabling the system to measure the total force applied on each PM. The rods were used to define the normal PM position, ensuring a comparable force on both PMs. The construction and function of

these rods has been described previously (18).

Six C-rings were individually sutured onto the following chords: anterior strut chord; anterior marginal chord; posterior intermediate chord; stem of the posterior marginal chord; basal posterior chord; and commissural chord (Fig. 1). The selected commissural chord was inserted near the annulus of the valve, but not to the tip of the leaflet. It was not possible to attach all C-rings onto chords extending from a single PM due to spatial constraints that might cause C-ring entanglement.

Experimental protocol

The atrial board containing the sutured mitral valve was positioned in the left heart simulator, and the C-ring cables were connected to the in-house C-ring signal conditioner. The PMs were attached to the force rods, and the left heart simulator was then filled with 0.9% saline solution. All signals from transducers and C-rings were zeroed and connected to a laptop computer through an in-house interface box. An in-house data collection program based on LabVIEW 5.0 was used to store the flow, pressure, and chordal force curves. This software stored data representing 10 cardiac cycles for each variable; these measurements were then averaged offline.

After preparing the system, the valve was placed in the normal PM position (1), which was defined by:

Basal-apical location: The PM rods were moved towards the annulus to a point where slack was observed in all chordae tendineae. The PM force rods were zeroed at this location. Each force rod was pulled backwards until a change in voltage of 0.02 V (0.09 N) was achieved for that particular rod. This was the minimal significant change that may be observed by the system. This defined a position with no slack or apparent stretching on the chordae tendineae.

Lateral location: The PMs arranged parallel to each other and directly aligned with the valve's annulus on each commissure. The commissural chords inserting in the annulus were vertically perpendicular to the annu-

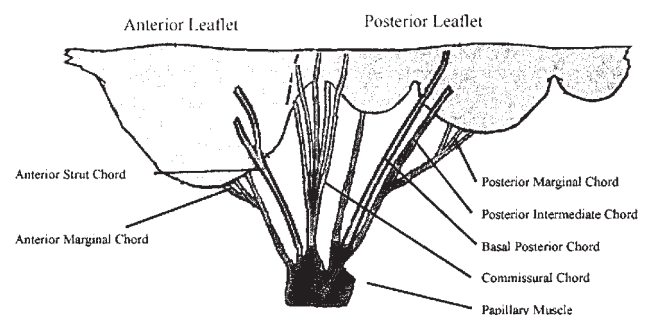


Figure 1: Schematic diagram of an extended mitral valve, identifying the chordae tendineae selected for tension measurements.

lar plane.

Septal-lateral location: The rods were moved septal-laterally until an even extension of the commissural chords inserting into the annulus was observed. Normally, this point was approximately 2 mm below the annular height midpoint.

Valve function in the normal PM position was confirmed under pulsatile flow by observing appropriate leaflet coaptation.

The simulator was run under physiological conditions, with the valve in the normal position (cardiac output 5 l/min; peak transmitral pressure 120 mmHg; heart rate 70 bpm; systolic duration ca. 300 ms). Flow, tension and pressure curves were stored and then processed offline.

After the initial set of recordings, the PMs were displaced to seven different PM positions. All displacements were symmetrical; therefore, both PMs were displaced equally to reach each position. Only symmetric positions were tested because it was not possible to attach all six C-rings on the same PM. The eight different positions are listed in Table I, with their corresponding vectorial displacements from the normal position. A schematic of the spatial reference system is shown in Figure 2. All recordings were repeated for all the different PM positions maintaining the physiological flow and pressure conditions previously described.

Statistical analysis

All data were reported as mean \pm SD, unless otherwise stated. Percentile differences were calculated using measurements in the normal PM position as reference, unless otherwise stated. Significance in percentile differences in force associated with repositioning of the PMs was compared using the one-sample Wilcoxon test. The two-sample Mann-Whitney test was used to compare porcine and human mitral valve populations. A p-value ≤ 0.05 was considered to be statistically significant. All statistical analyses were carried out using Minitab (version 14) software.

Results

The chordae tendineae tension curves were seen to follow the transmitral pressure curve for all valves. All valves coapted correctly, with no observable regurgitation orifices in the normal PM position. Chordal force was compared using peak systolic tension (PST) values for individual chords. The tension present on the individual chord during diastole was considered as the baseline (18).

PST measurements under 0.01 N were discarded because they could not be distinguished from electrical crosstalk. The C-rings were calibrated before and after the experiment to assess transducer functionality. Measurements for individual chords were discarded if the transducer showed malfunction in post-experimental calibration. Data for positions 005 and 505 were not obtained for all experiments due to geometrical restriction in the PM displacement apparatus. This restriction related to valves which had posteriorly inclined normal PM positions because of anatomical features of the valve. Only these factors account for the reduced number of specimens in some data sets; no other criterion was used to discard measurements.

PST values for porcine and human mitral valves

PST values for porcine and human mitral valves were compared; a summary for the two groups is listed in Table II for the normal PM position. Statistical analysis showed that there was no significant difference between the two groups for any of the six chordae tendineae in any of the PM positions used.

Variation in PST due to PM displacement

For all chords, percentage variations in PST used as reference the normal PM position, unless otherwise stated. A summary of PST results in the normal PM position is listed in Table III.

Anterior strut chord

The average force on this chord was 1.12 ± 0.53 N in

Table I: Vectorial composition of the different papillary muscle (PM) positions.

PM position	Displacement (mm)		
	Apical	Lateral	Posterior
000	0	0	0
005	0	0	5
050	0	5	0
055	0	5	5
500	5	0	0
505	5	0	5
550	5	5	0
555	5	5	5

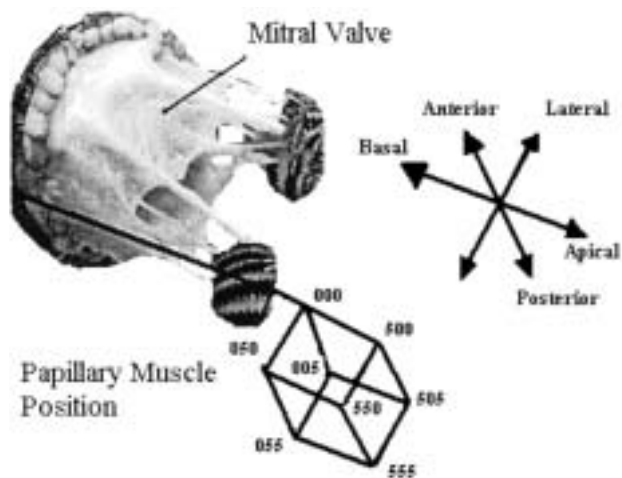


Figure 2: Spatial reference system based on the normal papillary muscle position. The vertices of the cube represent the eight different experimental positions used in the study.

the normal PM position. When the PMs were moved to positions 005, 050 and 055, PST did not vary significantly from that measured in the normal position. In contrast, significant ($p \leq 0.05$) increases in PST of $40 \pm 23\%$, $43 \pm 24\%$ and $39 \pm 33\%$ were observed when the PMs were moved to positions 500, 550 and 555, respectively. When comparing positions 505 and 500, there was a decrease in tension ($p \leq 0.05$), whereas the apparent increase when comparing positions 505 and 005 was not statistically significant ($p = 0.1$).

Posterior intermediate chord

The average PST on this chord in the normal position (0.34 ± 0.29 N) decreased by $37 \pm 10\%$ with the posterior displacement of the PMs in position 005. Position 500 showed a significant increase in tension of $105 \pm 68\%$ when compared to tension present in the normal PM position. Similarly, the tension had a significant ($p < 0.05$) increase for position 550. Although there was an apparent reduction in PST when going from position 500 to 505, this result was not statistically significant.

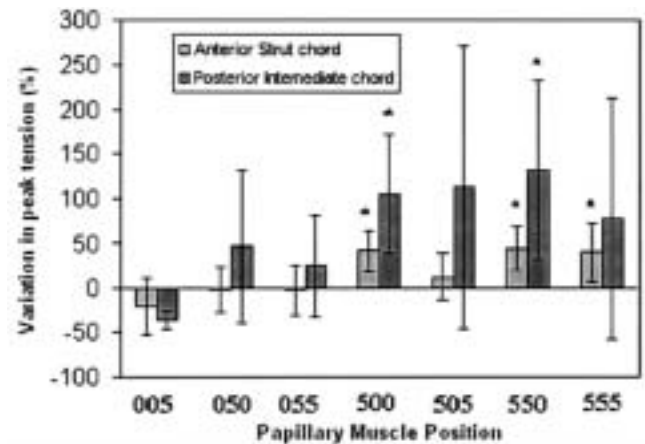


Figure 3: Variations in peak systolic tensions of different papillary muscle (PM) positions for the anterior strut chord and posterior intermediate chord. Bars represent mean \pm SD. *, different PM positions versus normal PM position ($p \leq 0.05$).

Position 555 showed a similar tension (0.37 ± 0.36 N) to that present in the normal PM position. The average variations in PST for the anterior strut chord and posterior intermediate chord are shown in Figure 3.

Anterior marginal chord and posterior marginal chord

For the anterior marginal and posterior marginal chords, there was no significant ($p > 0.05$) difference in PST for any of the PM positions used, with the exception of position 550 for the anterior marginal chord. The PST for these chords was relatively uniform for all positions (Fig. 4).

Basal posterior chord

For the basal posterior chord there were six different positions with statistically significant variations in tension. Positions 005, 055 and 050 showed significant decreases in PST of $40 \pm 16\%$, $43 \pm 22\%$ and $20 \pm 20\%$, respectively, when compared to the PST present in the normal PM position (0.21 ± 0.18 N) (Fig. 5). In contrast, PM relocation to position 500 increased the force by

Table II: Average chordae tendineae peak systolic tension (PST) values for human and porcine mitral valves in the normal papillary muscle position.

Chord	PST (N)	
	Porcine	Human
Anterior strut	1.02 ± 0.61	1.16 ± 0.57
Posterior intermediate	0.43 ± 0.48	0.30 ± 0.18
Anterior marginal	0.26 ± 0.18	0.41 ± 0.23
Posterior marginal	0.29 ± 0.30	0.25 ± 0.25
Basal posterior	0.21 ± 0.27	0.22 ± 0.14
Commissural	0.06 ± 0.03	0.21 ± 0.27

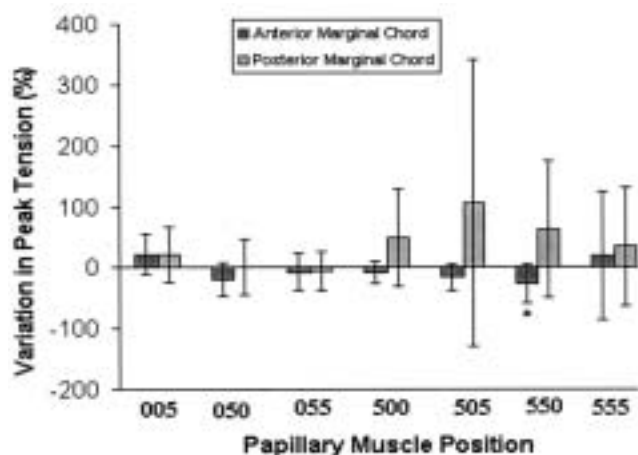


Figure 4: Variations in peak systolic tensions of different papillary muscle (PM) positions for the anterior and posterior marginal chords. Bars represent mean \pm SD. *, different PM positions versus normal PM position ($p \leq 0.05$).

107 \pm 45%, whereas relocation to position 550 induced an increase in tension of 109 \pm 50%. Position 555 also showed an increase in tension, though this variation was smaller than those observed in positions 500 and 550. When comparing positions 500 and 505, there was a decrease in tension of 30 \pm 9% associated with the posterior motion of the PMs ($p \leq 0.05$).

Commissural chord

The commissural chord showed high sensitivity to PM displacement (Fig. 5). Positions 005, 050 and 055 showed decreases in PST of 60 \pm 17%, 38 \pm 17% and 30 \pm 28%, respectively, when compared to the PST in the normal PM position (0.15 \pm 0.21 N). In contrast, positions 500, 505, 550 and 555 had increases in force of 114 \pm 52%, 153 \pm 110%, 104 \pm 58% and 104 \pm 93%, respectively. All of these variations were statistically significant ($p \leq 0.05$).

When comparing PST for different PM positions for each individual chord, the results showed the smallest percentage standard deviation in PST for the posterior

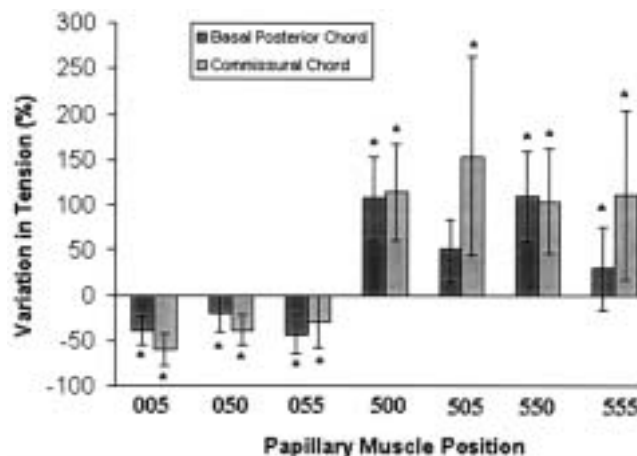


Figure 5: Variations in peak systolic tensions of different papillary muscle (PM) positions for the basal posterior chord and commissural chord. Bars represent mean \pm SD. *, different PM positions versus normal PM position ($p \leq 0.05$).

marginal chord ($\pm 15\%$). The anterior marginal chord also showed a relatively small variation from the average PST for all positions ($\pm 20\%$). The anterior strut had a percentage standard deviation of $\pm 28\%$, and the posterior intermediate chord of $\pm 48\%$ from the force present in the different PM positions. The largest variations in PST for the different PM positions were present in the basal posterior ($\pm 56\%$) and commissural ($\pm 61\%$) chords.

Discussion

During the cardiac cycle, the mitral valve is held within a very dynamic environment which is described by annulus displacement, ventricular motion and PM contraction. Within this environment, the basal chords maintain a relatively constant distance from the tips of the PMs to the annulus (9,19), aiming to maintain overall valve geometry and isolating the motion of the leaflets from the surrounding environment movement. The geometrical and anatomical construct of the mitral valve must ensure that the chords controlling coaptation - and especially those involved in the appropriate sealing of the valve - are less sensitive to the changing environment. Therefore, as expected, the intermediate chords were less sensitive to changes in PM position than the basal chords, whereas the marginal chords were the least sensitive of all chordal types to PM position variations. These characteristics were clearly shown by the standard deviations of the forces of the chords when different PM positions were compared. In addition, the direction of displacement of the PMs was directly related to which chord type presented altered tensions. Apical displacement affected tension on the secondary chords of both

Table III: Average chordae tendineae peak systolic tension (PST) values for the normal papillary muscle position.

Chord	PST (N)*
Anterior strut	1.12 \pm 0.53
Posterior intermediate	0.34 \pm 0.29
Anterior marginal	0.36 \pm 0.22
Posterior marginal	0.26 \pm 0.24
Basal posterior	0.21 \pm 0.18
Commissural	0.15 \pm 0.21

*Values include forces from both porcine and human mitral valves.

leaflets, whereas posterior displacement tended to reduce the force on chords which inserted into the posterior leaflet. The tensions on chords which inserted near the annulus were affected by displacement of the PMs in all directions.

The PSTs measured for different PM positions in the present study were at variance with those reported in a previous in-vitro investigation (16). These differences may be attributed to variations in the PM displacements used in the two studies, and to the use of glutaraldehyde to preserve the valve in the aforementioned study, as this has been shown to affect valve mechanics (17). The average PSTs for the primary (marginal) and secondary (intermediate) chords in the defined 'as-normal' PM position were within ranges observed previously in vivo in animal studies (19).

Apical displacement significantly increased the tension present on the anterior strut chord. When the PMs are displaced apically, the coaptation geometry of the mitral valve changes. Apical displacement generates tented leaflet geometries, as shown herein and in previous studies (1,21,22). Under a tented geometry, the intermediate chords restrict leaflet motion, and therefore these chords should hold most of the load during valve closure. The results of the present study for the anterior strut chord were in clear agreement with the aforementioned phenomenon, as apical displacement of the PMs tented the leaflets and significantly increased the load on the anterior strut chord. The decrease in force when repositioning the PMs from position 500 to position 505 was probably related to a redistribution of the load between chords.

Posterior PM displacement decreased the tension on the posterior intermediate chord by approximately 37%. This PM relocation shifted the coaptation line posteriorly, reducing the area of the orifice covered by this leaflet and decreasing the insertion angle of this chord. Both of these changes reduced the resultant force vector. The increase in tension associated with position 500 is explained by the same tenting described for the anterior strut chord. Combined apical-lateral displacement induced a significant increase in tension due to tenting of the leaflet and the stretching and redirection of the posterior intermediate chord. This effect was reduced in position 555 because of the posterior motion associated with this position.

The force on the anterior marginal chord and posterior marginal chord was relatively homogeneous for the different PM positions. As the marginal chords control coaptation in the tip of the leaflet, tension in them may be less sensitive to changes in PM position as the mitral valve is designed to operate in a highly dynamic environment. In addition, the tension measurements for these chords were small in magnitude and highly variable from valve to valve; thus, small

variations in force in these chords may not be detected by the methods used in the present study.

The tension on the posterior basal chord was highly sensitive to PM displacement. Posterior displacement reduced the tension on the posterior basal chord as it redirected the angle of the chord. This motion reduced the septal lateral component of force, and thus, reduced the overall resultant force. As chordae tendineae have a non-linear mechanical response to elongation (23,24), apical displacement increased PST on the basal posterior chord because of pre-straining. A pre-strained chord will be subjected to a higher tension for a similar strain during coaptation. Lateral displacement of the PMs reduced the force on the basal posterior chord. This reduction was probably due to a redistribution of the load with other chords.

The commissural chord selected for these experiments inserted near the annulus and below the septal-lateral midpoint of the valve (posterior section of the valve); therefore, trends in force variation due to PM displacement were similar to those present in the basal posterior chord. Similarly, pre-straining increased the force on the basal posterior chord during apical motion of the PMs. In addition, both posterior and lateral relocation of the PMs decreased the force on these chords. The relative contributions of these motions (lateral-posterior) to the force on the commissural chord should be different than the contributions to the force of the basal posterior chord because of their different angle and location of insertion on the valve.

The absolute tension on the chordae tendineae has two different contributors: a baseline tension which is dependent on the static tethering of the chords; and a dynamic component which is the result of valve motion due to transvalvular pressure. The forces measured in the present study were only those associated with transmitral pressure, as the diastolic force was considered to be baseline. The tethering component of the force can be observed in baseline shifts when repositioning the PMs. Although electrical drift in the transducers was small, the tethering force was not measured since stress relaxation due to the viscoelastic nature of the chords induced baseline shifts which are significant during the course of an 8-h experiment. In addition, this tethering tension is highly dependent on the force resulting from PM contraction. To the present authors' knowledge, no accurate measurements have been made of this force during the cardiac cycle. Hence, future research will be directed towards developing a protocol that will allow the absolute tension on these chords to be measured precisely.

In the native mitral valve, the annulus has a saddle-shaped geometry which varies in curvature during the cardiac cycle (25,26). In addition, this shape has been shown in the present authors' laboratory to have sig-

nificant effects on chordal force distribution; thus, it may appear that using a flat annulus is not physiological. The shape of the annulus is complex to mimic; hence, the use of a saddled annulus may introduce model-dependent artifacts and would complicate any analysis of the data. The flat annulus was selected because in pathologies such as ischemic mitral regurgitation and dilated cardiomyopathy (which are related to PM displacement), there is a flattening of the annulus, as shown previously (25,27). Furthermore, when the ventricle is dilated it is commonplace to find a dilated annulus. In order to correct annular dilation, an annuloplasty ring may be implanted, but the presence of these rings tends to decrease annular dynamics and lead to flattening of the valve. The use of a flattened annulus in the present study was related to conditions that may be found in the mitral annulus under pathologies which may lead to PM relocation.

Study limitations

There were several limitations associated with both the model and the procedure. The principal limitation was low number of human mitral valves, though this was partly compensated by the inclusion of porcine valves to increase the sample population. In addition, the use of porcine mitral valves allowed the comparison of force distribution among species. Chordal origin pattern in the PMs and branching characteristics varies widely among humans. Only human mitral valves with simple chordal origin patterns were used in the present study because they may be easily adapted to the left heart simulator, and thus can be better compared to porcine valves.

The results showed no significant differences in chordal force distribution between porcine and human mitral valves of similar sizes, thereby providing further evidence of mechanical similarity between the mitral valves of these species. However, further research on this topic is warranted as the geometry of the chords and insertion pattern is known to vary between these two species.

The left ventricle heart simulator has several limitations, despite its successful use in pioneering studies (11,13,18). Although the pressure and flow conditions generated in the loop are physiological, the simulator does not reproduce phenomena such as ventricular, atrial or PM contractions. Annular displacement was also not simulated; this is an important factor that affects chordae tendineae function, especially of those that insert near the annulus. Therefore, absolute values in tension of the posterior basal and commissural chords may have been lower than those present in the heart.

As outlined above, several pathologies associated with PM malfunction and ventricular remodeling may

displace the PMs, leading to mitral regurgitation (1,10,15), with the effects of PM displacement being transmitted to the leaflets through the chords. The results of the present study may provide surgeons with further understanding of how the different chords are affected as a result of different PM displacements. Moreover, this knowledge may allow the design or improvement of repair procedures aimed at restoring mitral valve function in pathologies associated with PM relocation.

In conclusion, although the simulator limitations did not allow the replication of all characteristics of mitral valve mechanics, the study results revealed the effects of PM displacement on the PST present on different types of chordae tendineae. Apical motion increased PST on the secondary chords, whereas chords on the posterior side of the valve were subject to a reduction in PST after posterior motion of the PMs. Chords which insert near the annulus were affected by lateral, posterior and apical displacement of the PMs. It is clear that further investigations are required to corroborate the initial findings of this study. The study results also showed that variation in tension due to PM relocation decreased with increasing distance of chordal insertion from the mitral annulus. Chords which insert near the annulus are the most sensitive to variations in PM position, whereas chords which insert into the tip leaflet are the least sensitive to PM relocation.

Acknowledgements

These studies were supported by a grant from the Heart Lung and Blood Institute, NIH (grant # HL52009).

References

1. He S, Jimenez JH, He Z, Yoganathan AP. Mitral leaflet geometrical perturbations with papillary muscle displacement and annular dilation: An in-vitro study of ischemic mitral regurgitation. *J Heart Valve Dis* 2003;12:300-307
2. Nielsen SL, Nygaard H, Fontaine, Hasenkam JM, He S, Yoganathan AP. Papillary muscle misalignment causes multiple regurgitation jets: An ambiguous mechanism for functional mitral regurgitation. *J Heart Valve Dis* 1999;8:551-564
3. Kinney EL, Frangi MJ. Value of two-dimensional echocardiographic detection of incomplete mitral leaflet closure. *Am Heart J* 1985;109:87-90
4. Kaul S, Pearlman JD, Touchstone DA, Esquivel L. Prevalence and mechanism of mitral regurgitation in absence of intrinsic abnormalities of the mitral leaflets. *Am Heart J* 1989;118:963-972
5. Kaul S, Spotnitz WD, Glasheen WP, Touchstone DA. Mechanism of ischemic mitral regurgitation:

- An experimental evaluation. *Circulation* 1991;84:2167-2180
6. Gorman JH, III, Gorman RC, Jackson BM, et al. Distortions of the mitral valve in acute ischemic mitral regurgitation. *Ann Thorac Surg* 1997;64:1026-1031
 7. Perloff JK, Roberts WC. The mitral apparatus. Functional anatomy of mitral regurgitation. *Circulation* 1972;46:227-239
 8. Kono T, Sabbah HN, Rosman H, Alam M, Jafri S, Goldstein S. Left ventricular shape is the primary determinant of functional mitral regurgitation in heart failure. *J Am Coll Cardiol* 1999;20:1594-1598
 9. Ojtsuji Y, Handshumacher MD, Schwammenthal E, et al. Insights from three-dimensional echocardiography into the mechanism of functional mitral regurgitation: Direct in vivo demonstration of altered leaflet tethering geometry. *Circulation* 1997;96:1999-2008
 10. Gorman JH, III, Jackson BM, Gorman RC, Kelly ST, Gikakis N, Edmunds H. Papillary muscle discoordination rather than increased annular area facilitates mitral regurgitation after acute posterior myocardial infarction. *Circulation* 1997;96(suppl.II):II-124-II-127
 11. Madu EC, Baugh DS, Cruz IA, Johns C. Left ventricular papillary muscle morphology and function in left ventricular hypertrophy and left ventricular dysfunction. *Med Sci Monit* 2001;7:1212-1218
 12. Liel-Cohen N, Guerrero JL, Otsuji Y. Design of a new surgical approach for ventricular remodeling to relieve ischemic mitral regurgitation: Insights from three-dimensional echocardiography. *Circulation* 2000;101:2756-2763
 13. Moanie SL, Guy S, Gorman JH, et al. Infarct restraint attenuates remodeling and reduces chronic ischemic mitral regurgitation after postero-lateral infarction. *Ann Thorac Surg* 2002;74:444-449
 14. Messas E, Guerrero JL, Handschumacher MD, et al. Chordal cutting. A new therapeutic approach for ischemic mitral regurgitation. *Circulation* 2001;104:1958-1963
 15. He S, Lemmon JD, Weston MW, Jensen MO, Levine RA, Yoganathan AP. Mitral valve compensation for annular dilation: In-vitro study into the mechanisms of functional mitral regurgitation with an adjustable annulus model. *J Heart Valve Dis* 1999;8:294-302
 16. Nielsen SL, Nygaard H, Fontaine AA, et al. Chordal force distribution determines systolic mitral leaflet configuration and severity of functional mitral regurgitation. *J Am Coll Cardiol* 1999; 33:843-853
 17. Jensen MO, Lemmon JD, Gessaghi VC, Conrad CP, Levine RA, Yoganathan AP. Harvested porcine mitral xenograft fixation: Impact on fluid dynamic performance. *J Heart Valve Dis* 2001;10:111-124
 18. Jensen MO, Fontaine A, Yoganathan AP. Improved in vitro quantification of the force exerted by the papillary muscle on the left ventricular wall three dimensional force vector measurement system. *Ann Biomed Eng* 2001;29:406-413
 19. Lomholt M, Nielsen SL, Hansen SB, Andersen NT, Hasenkam JM. Differential tension between secondary and primary mitral chordae in acute in-vivo porcine model. *J Heart Valve Dis* 2002;11:337-345
 20. Otsuji Y, Handschumacher MD, Liel-Cohen N. Mechanism of ischemic mitral regurgitation with segmental left ventricular dysfunction: Three-dimensional echocardiographic studies in models of acute and chronic progressive regurgitation. *J Am Coll Cardiol* 2001;37:641-648
 21. Godley RW, Wann LS, Roger EW. Incomplete mitral leaflet closure in patients with papillary muscle dysfunction. *Am Heart J* 1979;97:312-321
 22. Dent JM, Spotnitz WD, Nolan SP. Mechanism of mitral leaflets excursion. *Am J Physiol* 1995;269:H2100-H2108
 23. Sedransk KL, Allen JG, Vesely I. Failure mechanics of mitral valve chordae tendineae. *J Heart Valve Dis* 2002;11:644-650
 24. Liao J, Vesely I. A structural basis for the size-related mechanical properties of mitral valve chordae tendineae. *J Biomech* 2003;36:1125-1133
 25. Kaplan SR, Bashein G, Sheehan FH, et al. Three-dimensional echocardiographic assessment of annular shape changes in the normal and regurgitant mitral valve. *Am Heart J* 2000;139:243-250
 26. Timek TA, Miller DC. Experimental and clinical assessment of mitral annular area and dynamics: What are we actually measuring? *Ann Thorac Surg* 2001;72:966-974
 27. Flachskampf FA, Chandra S, Gaddipatti A, et al. Analysis of shape and motion of the mitral annulus in subjects with and without cardiomyopathy by echocardiographic 3-dimensional reconstruction. *Am Soc Echocardiogr* 2000;13:277-287